

Research article

Developing an Intelligent Farm System to Automate Real-time Detection of Fungal Diseases in Mushrooms

Chatklaw Jareanpon, Suchart Khummanee*, Patharee Sriputta and Peter Scully

Department of Computer Science, Faculty of Informatics, Maharakham University, Maharakham, Thailand

Curr. Appl. Sci. Technol. 2024, Vol. 24 (No. 1), e0255708; <https://doi.org/10.55003/cast.2023.255708>

Received: 26 August 2022, Revised: 6 January 2023, Accepted: 18 April 2023, Published: 1 June 2023

Abstract

Keywords

fungal disease;
smart farming;
precise intelligent farming;
innovative farm;
Internet of Things (IoT);
robotics;
deep learning;
Sajor-caju mushroom

Mushrooms are economically valuable crops of high nutritional value. However, during cultivation they are continually threatened by fungal diseases, even in controlled-condition farm ecosystems. Fungal diseases significantly affect mushroom growth and can rapidly contaminate an entire crop. Farmer inspections can be hazardous to farmer health. This paper contributes an automated fungal disease detection system for the Sajor-caju mushrooms together with an intelligent farm system for precise cultivation environment control. The objective was to create and test a detection system that could detect fungal diseases rapidly, reduce farmer exposure to fungal spores, and alert farmers when fungal disease was detected. The system is composed of three parts: (i) a high-precision environment control system, (ii) an innovative imaging robot system, and (iii) a real-time fungal disease prognosis system using deep learning, with an alarm system. The trial results show that the real-time disease prognosis system has 94.35% precision (89.47% F1-score, $n=13,500$), and its twice daily inspections detect and report fungal disease typically within 6 to 12 h. The innovative farm's overall capability for mushroom cultivation (environment control) is regarded as *excellent* and has *precise control* (99.6% capability, over 3-months). The innovative imaging robot's overall operational trial performance is *effective* (at 99.7%). Moreover, the system effectively notifies farmers via smartphone when a fungal disease is detected.

*Corresponding author: Tel.: (+066) 0848755582 Fax: (+066) 043754359
E-mail: suchart.k@msu.ac.th

1. Introduction

Mushrooms are a popular consumer food category providing a source of dietary nutrition including carbohydrates, proteins, fats, minerals, and vitamins [1, 2]. Consumption of some varieties have been linked to lowering levels of harmful cholesterol (low density lipoprotein) [3] and some have low sodium content, supporting their suitability for people with high risk of diseases such as liver, kidney and heart diseases, and hypertension.

Most commercially cultivated mushrooms in Thailand thrive in hot and humid climates and were traditionally harvested only during the warm and rainy seasons. The concept of closed-loop ecosystem environments for mushroom cultivation was introduced to provide higher yields necessary because of high demand. Modern intelligent farm systems [4-7] can manage, monitor, and optimize the environment for the cultivation of various crops, including mushrooms. They can control temperature, humidity, soil moisture, light, wind, carbon dioxide levels, and so on, using embedded microcontroller systems with various sensors and robotic actuators. The transition from traditional mushroom cultivation methods to smart methods allows for year-round cultivation and for increased yield (volume) of mushrooms. Yet, diseases can still occur even with closed-loop ecosystems, and fungal diseases are among the most damaging for mushrooms.

According to Kassim *et al.* [8] and Chieochan *et al.* [9], the leading causes of fungal disease in mushrooms are contamination of the cultivation material and the accumulated humidity inside the fruiting chamber during cultivation. The first cause can be solved by controlling the cleanliness of the cultivation material during the packing process. The second cause arises from natural fluctuations in environmental conditions. Mushrooms can grow well in a temperature range of 25-35°C and with a relative humidity of about 70-90% [1]. However, preferable temperature and relative humidity of each mushroom variety are varied. For example, the preferred temperature and relative humidity for the Sajor-caju mushroom during incubation and flowering periods are 25°C and 80-85%, respectively.

Within precision farming, there exists a known trade-off of precision environment condition control and energy consumption costs against product quality outcome and its marketable value. Often, broadening the range of acceptable conditions can lead to an economically-viable point of cost with product value, and allow for a system of carefully balanced factors that achieves an effective financial investment. Therefore, most smart farms define an acceptable range of environment conditions to reduce energy (compared to fixed conditions, for example permanent air conditioning), such as a temperature range of 25-28°C and humidity range of 80-85%. Yet, a consequence of loosening the environment control can be an accumulation of humidity and the realization of conditions in which fungal disease can then thrive.

The typical procedure for detection of fungal diseases in mushroom cultivation plots requires farmers to enter the fruiting chamber (environment) and visually inspect each planting bag. Additional inspection tasks include tracking growth, harvesting, and so on, often leading to 1 to 3 h per day in the environment. Inhalation of the micron-sized spores has been linked to (farmer) health concerns [10], including developing respiratory problems, such as pneumonitis, lung abscesses, lung diseases, kidney failures, cancer, chronic fatigue, and allergies. Therefore, reduction of time spent in the environment helps to mitigate the farmer health ailments.

Mushrooms, which are fungi, can be affected by fungal disease. Once a fungal disease begins to grow on a mushroom, it will suppress growth and will eventually consume the mushroom unless removed or treated. There are many fungal disease varieties that are colloquially known by terms such as “green fungus”, “yellow fungus”, “black fungus”, and so on. The typical pathway of fungal disease growth starts with contaminating fungal planting material and proceeds with accumulated moisture during mushroom cultivation [8, 9].

In this research, data on the Sajor-caju mushroom and the fungal diseases affecting consultant farmers in Khon Kaen and Maha Sarakham provinces of Thailand were collected. Special attention was paid to “green mold” or “green fungal disease” (*Trichoderma harzianum*) as it is a major source of contamination and crop loss for mushroom farmers, including the Sajor-caju variety [11]. Table 1 shows an example of the sequence of green fungal disease growth phases on Sajor-caju mushrooms. Throughout the fungal disease growth, fungal spores are released. Consequently, nearby mushrooms can rapidly become infected with the same fungal disease, and this poses a major problem for closed-loop ecosystem fruiting chambers. Within 48 h, all mushrooms in the fruiting chamber may become infected with the fungus. For these reasons, vigilance, and early detection of fungal diseases (within 12 h) can mitigate the massive potential of mushroom crop damage and loss.

Table 1. Examples of characteristics and duration of green fungal disease

Phase	Example of Fungal Disease	Description
1		Duration 1-6 h: Fungal disease occurs as a small spot (green colony) at the mouth of the planting bag. An area with accumulated moisture is visible.
2		Duration 7-12 h: Fungal disease begins to spread at the mouth of the planting bag. The mushroom continues to grow normally.
3		Duration 13-18 h: Fungal disease expands and begins to consume the mushroom.
4		Duration 19-24 h: Fungal disease has spread to most of the planting bag. Mushroom growth is stalling.
5		Duration 25-30 h: Fungal disease has spread to the entire planting bag. The fungal-infected mushroom has begun to turn brown.
6		Duration 31-36 h: Fungal disease has grown to one-third of the planting bag. The mushroom has stopped growing.
7		Duration over 36 h: Fungal disease has spread throughout the planting bag. The mushroom is dark brown and has stopped growing. The fungal disease is now mature.

This research work presents the design and evaluation of an innovative and intelligent farm system prototype for integrated mushroom cultivation (environment control) with innovative fungal disease detection. The end-to-end system includes farm design to farmer notification. The key contributions are the design and evaluation of:

1. An intelligent farm system with environment control system to cultivate Sajor-caju mushrooms optimally.
2. An innovative imaging robot for fungal disease detection.
3. A real-time automated fungal disease detection system using the imaging robot, a deep learning image-based model, and a notification system.

2. Materials and Methods

The automated system, which was our innovative farm, was installed at two sites in Khon Kaen and Maha Sarakham province, Thailand. The consultant Sajor-caju mushroom farms are in operation throughout the year, with stable and continuous high yield production. Every effort was made to ensure minimal interruption in the farming operations.

2.1 Requirements: automated system for cultivation and disease analysis

An intelligent farm system for mushroom cultivation and fungal disease diagnosis should have the following qualities:

1. Continuously monitor environment conditions such as temperature, humidity, light, and so on, via sensors.
2. Control environment conditions such as fogging (mist), air conditioning, lighting, exhaust fans, and so on, via actuators.
3. Respond to sensor conditions by activating control actuators.
4. Capture images to monitor farm and system operations.
5. Capture images from which fungal disease can be diagnosed and pinpointed.
6. Notify or alert farm operator(s) for disease diagnosis and system events.

Existing intelligent farm systems [3-6] and the consultant farms in this study have not been capable of fungal disease analysis. There are several reasons for this:

1. Ceiling or rack mounted surveillance cameras inside smart farms can often view the entire crop (Figure 1(A)); however, their directional perspective is unsuitable for disease analysis as they lack image clarity and target consistency, as shown in Figure 1(B).
2. Suitable images for fungal disease analysis are taken of the (air-exposed) front of the mushroom planting bag, shown in Figure 1(C), which is challenging to achieve consistently without automation (robotics).
3. Mushroom cultivation demands low light conditions, while high clarity photography for fungal disease analysis requires well-managed lighting.
4. Best practice guidelines recommend that farmers manually survey their crop for fungal disease at least twice daily, as disease can start at any time and spread to the entire crop within 12 h. As spore inhalation can be detrimental to farmer health, regular automated inspection and diagnosis is preferable.

Based on the previous work concerning the problems and limitations of intelligent mushroom cultivation and fungal disease diagnosis, we have designed, developed, and evaluated an automated system – *an innovative and intelligent farm*. The system uses (i) an environment control system to manage growing conditions, (ii) an imaging robot to regularly capture images for disease



Figure 1. Location of camera installations and photos taken from existing smart farms

analysis, (iii) a fungal disease detection system using a deep learning model, and (iv) a real-time alert service to inform farmers when fungal disease is detected and to monitor the farm conditions. As a result, the system aims to lower the farmers' time inside the fruiting chamber, lowering the farmers' risk of health complications and disease arising from spore inhalation.

2.2 Environment and environmental control system

The real innovative farm for mushroom cultivation from the study is shown in Figure 2. Each smart farm site consisted of one or more fruiting chambers, with uniform structure, design, and dimensions. The size of the fruiting chamber is 6.2 x 12.5 x 3.5 m (width x length x height). The front of the building is equipped with ventilation fans (sizes 36-50 inches). The rear of each fruiting chamber is equipped with a water pump (1.5 hp), an evaporative cooling panel (EVAP size as 5 x 6 x 1.8m), and includes a 200 L water tank, as shown in Figure 3(A).

The internal structure is a closed system and is equipped with insulation to maintain a constant temperature all year round. The fruiting chamber has a 330-watt solar panel (external roof), a solar control cabinet (Inverter), a 220-volt electrical system, and a lighting system. In addition, the fruiting chamber is equipped with temperature (DS18B20), humidity (TH-030), soil moisture, and light sensors, with each type of sensor installed in approximately six positions throughout the house, as shown in Figure 3(B). Surveillance cameras are installed at two or more locations inside the house to monitor the operation of various pieces of equipment such as fans, lighting and cooling system, etc. (Figure 3(D)).

The smart farm control room is located outside the fruiting chamber(s), consisting of the electrical system, the control system for all equipment, all the sensor receivers, and the computer system for the artificial intelligence and software systems (i.e., detection model, data receipt/storage, notification, and monitoring systems, etc.), as shown in Figure 3(E).

Microcontrollers and computer systems automatically control the electrical and IoT equipment across the innovative farm system (within the fruiting chambers). The environment control intelligence system is deterministic, and its objective is to control relative humidity and temperature within a nominal range. When the temperature sensor value exceeds the maximum range, the external extractor fan is initiated and will terminate after the temperature returns to nominal. When relative humidity falls below the lower threshold, the misting device (Figure 3(C)) will start and terminate after humidity returns to a nominal percentage.

The precise sensor value ranges for Sajor-caju cultivation varied among the consultant farmers, the status of their crops, location and other constraints. Temperature ranges included 28-32°C, 25-30°C, and precisely 25°C (Figure 3(F)). Relative humidity ranges were generally held with 60-80% or 60-70%. Light levels ranged from zero to very low light, which we calibrated at 20-30% on our sensors. The overall control system design is shown in Figure 4.



Figure 2. Smart farm structure

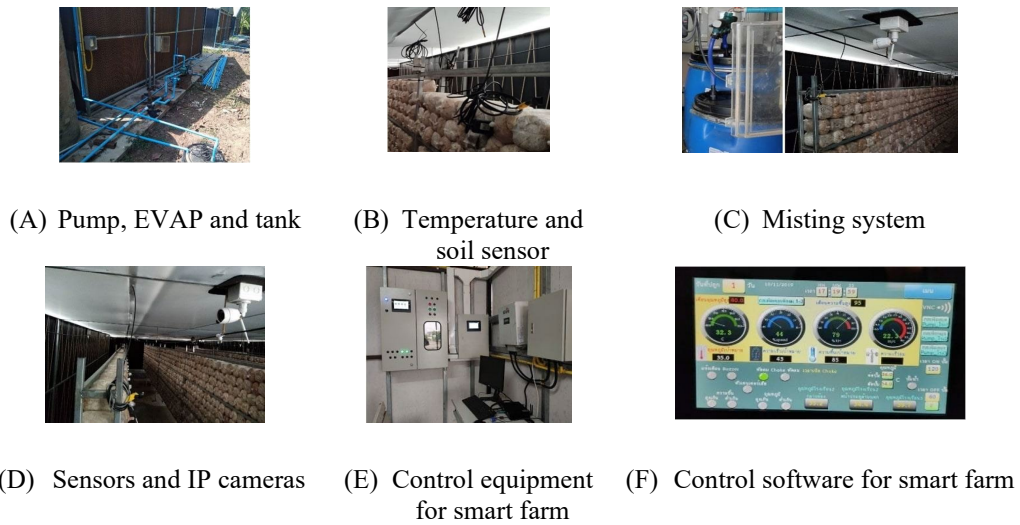


Figure 3. A real innovative farm for mushroom

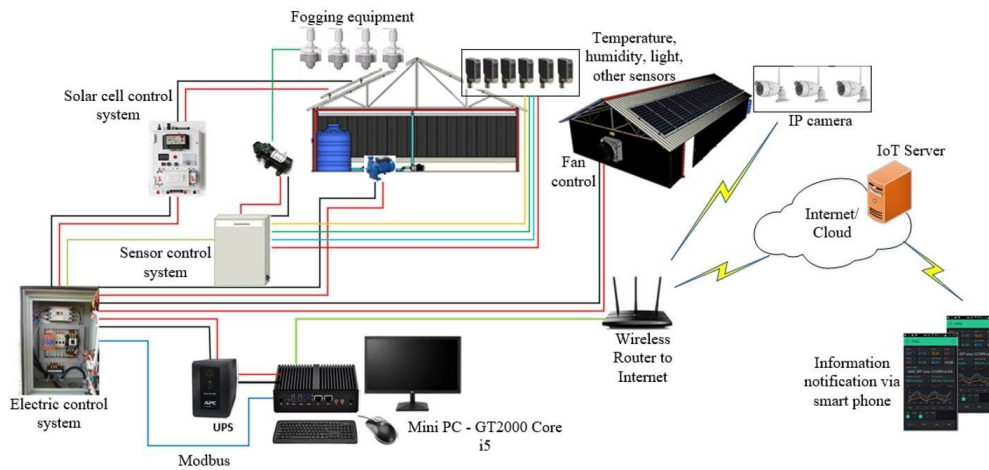


Figure 4. Overall control system design

2.3 Imaging robot design

The imaging robot is the component of the innovative farm system which passively captures images of the mushroom racks from which fungal disease can be identified. Given the problems and limitations of previous work concerning cultivation with fungal disease diagnosis (see Section 2.1), existing surveillance and static camera systems with limited lighting were inadequate, and a specialized camera solution was required. The requirements of this imaging task (see Section 2.1) are addressed by the automated imaging robot design described in this section.

The imaging robot's objectives are to (i) obtain high-clarity and high-definition images of the air-exposed mushroom surfaces (mounted in racks), (ii) reduce farmer exposure to spores, and (iii) mitigate the disturbance to crop conditions (to avoid impeding crop growth).

Further requirements of the imaging robot:

1. The robot must be able to capture clear images of the front of every mushroom planting bag.
2. Photographic lighting by the robot must not hinder mushroom cultivation.
3. The robot must automatically capture images of mushrooms throughout the day (24 h/day).
4. The robot must be small, lightweight, and flexible to operate.
5. The robot must be able to transmit captured images for image processing for fungal disease detection. Wireless communication is selected, as it reduces cabling weight, and thus reduces robot motor specification and improves the convenience of transporting and operating the robot.

The detailed criteria for the design and development of the imaging robot within the innovative farm are:

1. The robot moves in a "square wave" pattern to cover the image target capture area.
2. The robot can move horizontally (approximately 1 to 12 m distance in the X-axis direction) and vertically (1 to 2 m in the Y-axis direction) automatically by moving along the rails inside the smart farm (V-Slot aluminum profile).
3. The robot uses a collision sensor (Impact Switch Module) to automatically detect the end of its X- and Y-axis motion.
4. The movement speed of the robot can be adjusted according to requirements, by software adjustments.
5. The robot can capture images of various sizes; the images must be HD resolution (the default size is 1,280 x 720 pixels).
6. The image brightness (lighting) is created by an LED light bulb (1250 lumen, diffuse 6500K, IR- and UV-filtered). Empirical trials showed this brightness level and filtering as most suitable for image capture during mushroom cultivation.
7. The image data captured by the robot is transmitted over the wireless network.
8. Communication between the robot and the image processing system is carried out through an IP network.
9. The robot and the image processing system operate all day (24 h) because it is impossible to predict when a fungal disease will occur.

These criteria lead to the following robot design and development steps:

Step 1/4: Design a prototype robot within 3D design software [9] to simulate the operation and define the robot's various components, as shown in Figure 5.

Step 2/4: Build the rail system to allow the imaging robot to move in a predetermined range. The rail's material should be small, lightweight, strong, and inexpensive. Therefore, aluminum profiles are used to build the rail system, as shown in Figure 6.



Figure 5. Designing a prototype robot using 3D design software [12]

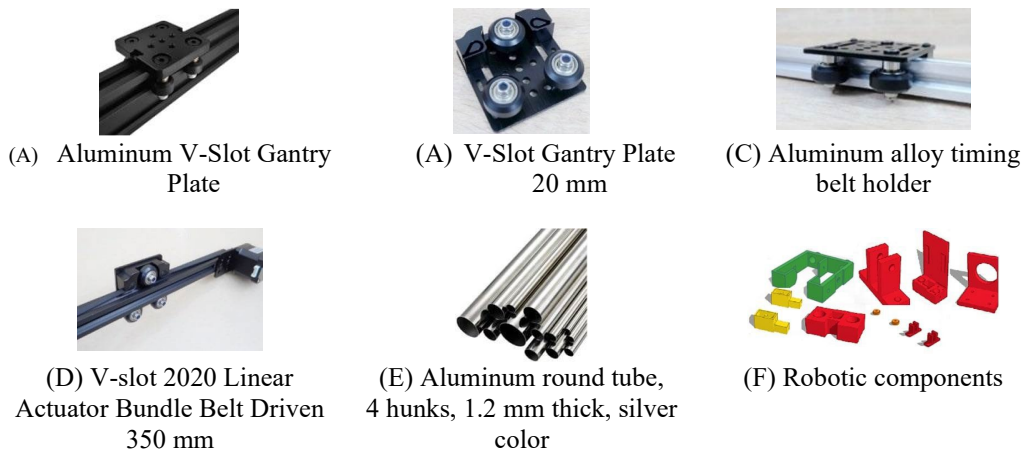


Figure 6. Materials used for the construction of the rail system

The completed rail system is shown in Figure 7. The horizontal (X-axis) rails within the fruiting chamber are approximately 12 m long (left-to-right of mushroom rack), and the vertical rails (Y-axis) are approximately 2 m long (height). The movement of the robot (X and Y-axis direction) uses a belt system (size 6-8 mm) with stepper motors controlled by a microcontroller (Arduino UNO). The movement speed of the robot on the rail can be customized according to the requirements.

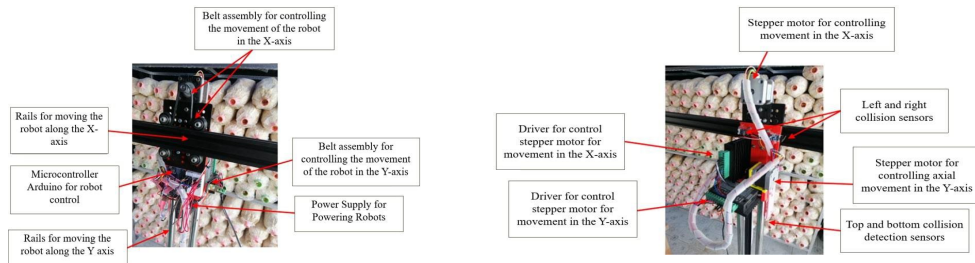


Figure 7. Overview of the imaging robot

The imaging robot traverses a repeating “square wave” pattern from the starting (left) position of the rack to the end (right) position of the rack. Each individual cycle of the wave pattern (depicted by Figure 8(A)) takes approximately 1.9 min to complete, including horizontal and vertical movement time and 12 image captures (each marked by red asterisks within Figure 8(A)). The robot’s traversal time per cycle is calculated as $2*X + 14*Y + 12*P = 2*6\text{ s} + 14*3\text{ s} + 12*5\text{ s} = 1.9\text{ min}$. Where (X) corresponds to X-axis movement time (6 s), (Y) is Y-axis movement time (3 s), and (P) is the capture time (5 s).

The robot is fitted with an IPC-V380-IPC camera with a horizontal field of view (HFOV) between 60-90 degrees. Empirical trials led us to a suitable target distance of 60 cm with lighting brightness at 1250 lumens (12-watt) for capture at 1080P and 720P, shown in Figure 8(B). The camera lens’s relatively wide HFOV enables wide capture shots which reduces the time taken for capture events and their lighting time (P); however, this causes the image edges to distort. To mitigate the distortion blur, the captured images have approximately 15% overlap (108 x 230 pixels) (Figure 8(C)). The size of the actual image (including overlap) corresponds to approximately 33.87 cm in width and 17.06 cm in height.

Previous studies [2, 9, 13] showed that short periods of light stimulate mushroom tissue formation. This provides some evidence that the image capture process is likely to be beneficial to the mushroom cultivation; however, a yield measurement impact study of this factor caused by our imaging robot, will require further study.

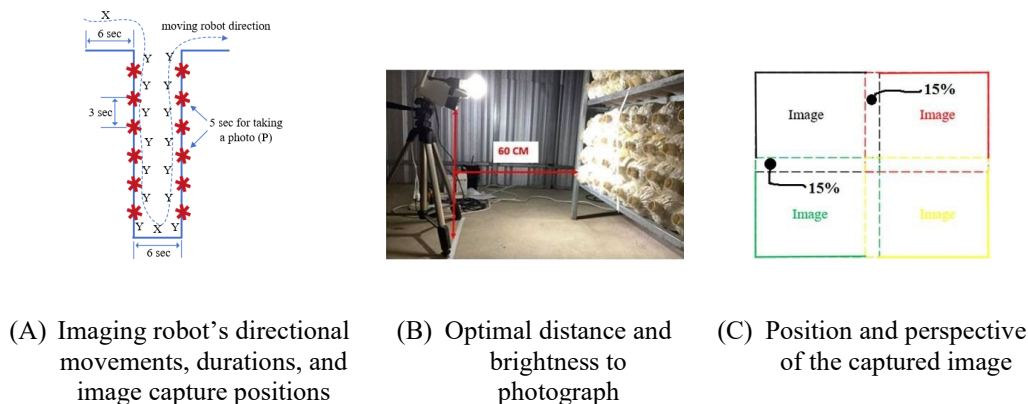


Figure 8. Imaging robot traversal pattern and image capture conditions

Step 3/4: Install the imaging robot onto the rails. The imaging robot is composed of a microcontroller, sensors, actuators (stepper motors), IP camera, lighting system, and other equipment. Each attached composite device has a function, which are listed in Table 2.

The assembled devices in Table 2 are pictured in Figure 9 – the imaging robot. Under actual image capture operation, the imaging robot is contained within a membrane or shielded box to extend system lifetime and prevent moisture ingress within the high humidity environment. The rails and mechanical contact parts are regularly checked for wear and residue/debris removal.

Step 4/4: Integrate the imaging robot component into the innovative farm system. The rail system and imaging robot are installed into the fruiting chamber, in front of the mushroom cultivation rack. One robot can photograph two mushroom racks. Two capture cameras and lighting systems are installed (back-to-back) onto the robot platform to capture two racks at once (shown in Figure 9(B)). Generally, one fruiting chamber (size 6 x 12 m) can contain about 3-4 mushroom racks, which requires 2 or 3 imaging robots.

Table 2. Imaging robot devices and their functions

Equipment	Device Name and Specification	Device Function
	Arduino ATmega328P, Operating Voltage 5V, UNO R3 type SMD	Control and operate sensor devices (Impact switches) and actuators (Stepper motors and LED light bulb)
	Stepper Motor 42BYGH47-401A Nema 17	Control the movement of the robot on the X and Y-axis
	Switch Collision Module Sensor (Impact Switch Module)	Determine the collision of the robot at the end of X and Y-axis movement (change direction of movement)
	TB6600 Stepper Motor Driver	Motor driver for driving stepper motors
	Timing belt width 6-8 mm for 3D printer	Used to force the robot to move in the X and Y-axis
	CCTV MODEL: IPC-V380-IPC AK type IP Camera: HD CAMERA V380-IPC 3	Photograph mushrooms at HD resolution (720p) and communicate over the Wi-Fi network.
	LED NEO LDAHV12DH5T 12w, 1250 lumen, 6500K color temp.	Lighting while the robot is taking pictures
	Adapter 2000mA (DC 5.5 x 2.5MM) 12V 5A	Power supply for microcontrollers, motors, and sensors
	Other accessories of CNC	Other accessories to assemble into a robot include nuts, screws, etc.



(A) The assembled imaging robot



(B) Imaging robot with two cameras and lighting

Figure 9. The assembled imaging robot for image capture, shown within a smart farm building

The robot's operation control algorithm is shown in Figure 10. The algorithm starts by defining variables (1) such as the robot's direction of movement, shooting time, collision state, etc. The next step (2) is to assign input and output signals to the various pins of the Arduino, such as the collision detection pin as the input and the motor control pin as the output pin. After assigning variables and pins to the microcontroller, the robot begins executing the "square wave" traversal pattern. Then, (3) the robot starts to move to the right (X-axis) first. When X-axis rail collision impact sensor triggers (the robot has reached the edge of the rail frame) (4), the robot will automatically begin moving back in the opposite direction (5). However, if no X-axis rail collision occurs, then the robot continues downward (6) in the Y-axis (always moving from top to bottom). If the robot collides with the bottom edge while moving downward, it immediately moves in the opposite direction (7), like the X-axis. If the robot's motion is normal, it triggers a lighting and image capture event, as shown in Figure 8(A). The images obtained at this phase are 720 pixels in width and 1280 pixels in length.

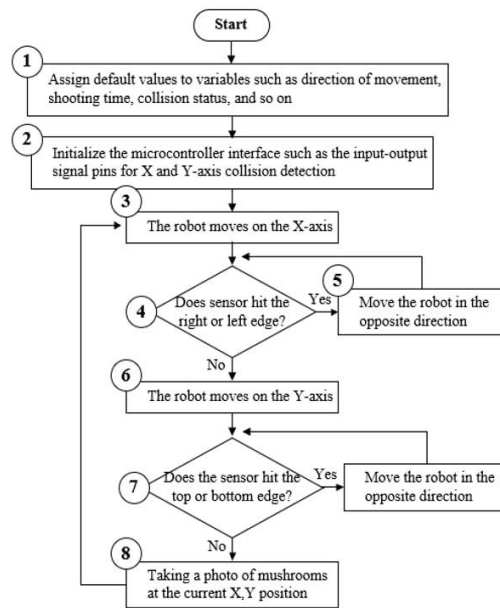


Figure 10. The algorithm for controlling the movement and shooting of the robot

2.4 Fungal disease detection modeling and real-time alert procedure

The images captured at Step 8 (Figure 10) are transferred into a deep learning process to identify the fungal disease and alert the farmer. The work leading to this detection system includes (i) image preprocessing, (ii) training deep learning models, and (iii) conducting predictive testing trials.

2.4.1 Image preprocessing

The images obtained (720 x 1,280 pixels) by the imaging robot undergo preprocessing operations, similarly to Ghavate and Joshi [14] and Pooja *et al.* [15]. Images are segmented according to the number of mushroom bags. Figure 11(A) shows 10 segmented images suitable for further image processing (shown by a square frame). Remaining pixels of the image that are not within the mentioned square are discarded.

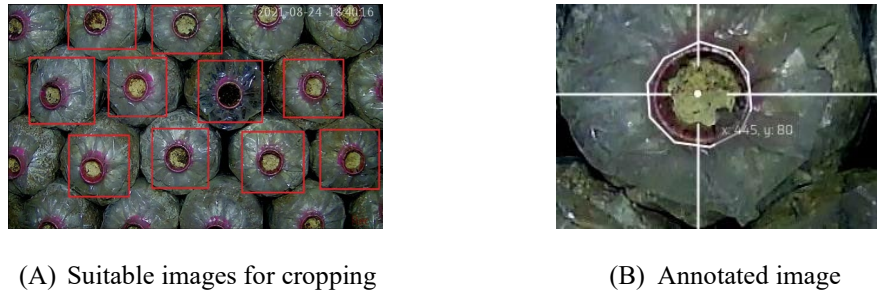


Figure 11. Examples of suitable images for cropping and annotated image

Step 1/2: Image segmentation using mask R-CNN. To achieve the image segmentation, we have followed the mask R-CNN method [16]. The first step is to annotate a point or region of interest in the source images. We use a point and circular region anchor annotation [17-19] to mark the center point of the mushroom planting bag within the images. This technique marks the position as an annotated polygon mask, as shown in Figure 11(B). These annotations are exported as JSON files. Next, the image and JSON file pairs are used for training and testing by Mask R-CNN (using ResNet101 as the default algorithm) to locate the image object. The total number of images used for the Mask R-CNN process is 250, divided into two groups: 200 images for training (80%) and 50 images for testing (20%). As a result, the objects of the image after Mask R-CNN processing are entirely shown in circles, as shown in Figure 12(C).

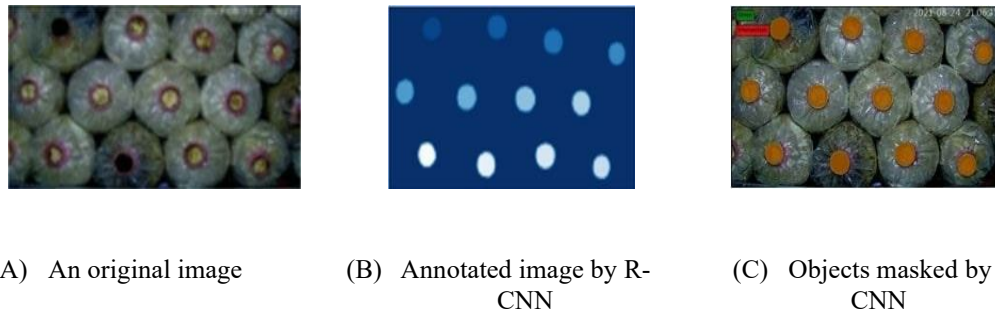


Figure 12. Examples of suitable images for cropping and annotated image

The results showed that the Mask R-CNN segmentation model can find all objects in the mushroom images. After locating the desired objects using the Mask R-CNN technique, the next step is creating bounding boxes around the objects. Each block has a size of 224 x 224 pixels (Figure 13(A)). Next is to crop those bounded boxes into sub-images (the front of the mushroom planting bag). The typical number of segmented sub-images is between 10 and 12 per original captured image, as shown in Figure 13(B).

Step 2/2: Collate images to train CNN models for fungal disease detection (prognosis). The segmented images are divided into two classes: (i) fungal disease images and (ii) non-fungal disease images, with 1,000 images per class. Each image class is divided into two groups, consisting of 800 training images (80%) and 200 testing images (20%). The training image group is further divided into two subgroups: 520 (65%) retained for training and 120 (15%) separated for model validation. The testing image group (200 images) is used to test the independent accuracy of the CNN models, depicted in Figure 14.

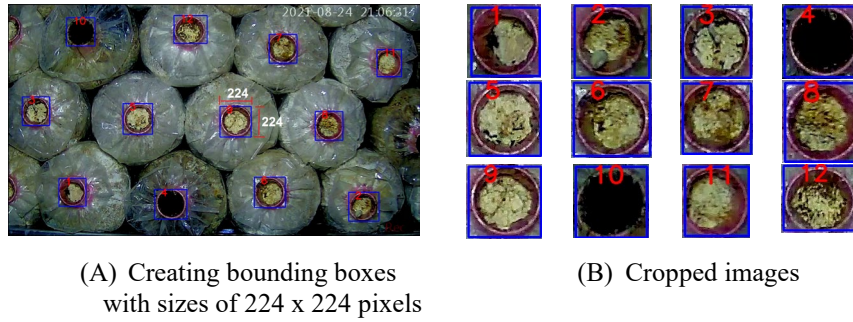


Figure 13. Creating bounding boxes and cropped (segmented) images

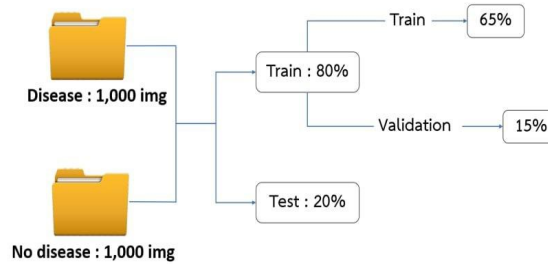


Figure 14. Clustering data to find a suitable CNN model in fungal prognosis

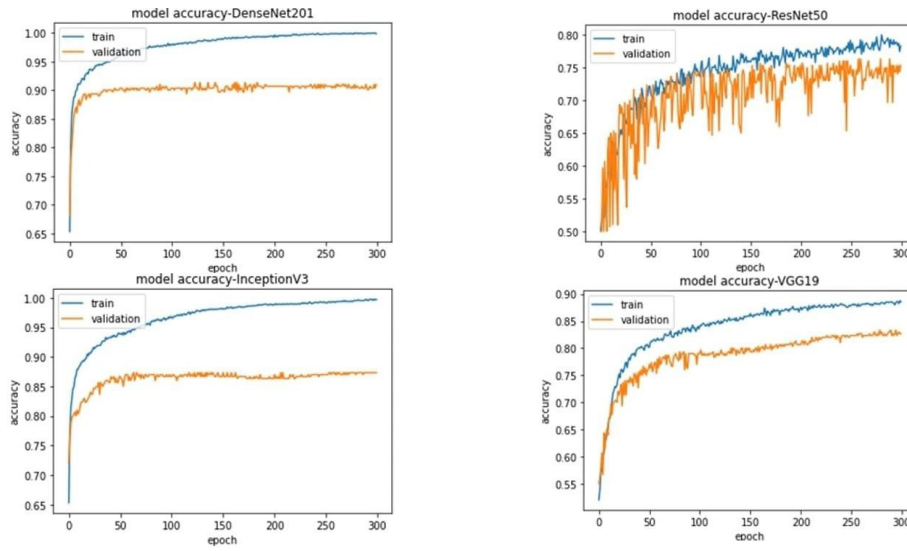
2.4.2 Model selection

This section presents the results of testing current and popular high-precision CNN models to determine which model has the highest accuracy in fungal disease detection and thus prognosis, using our collated image dataset. The CNN models trained in this research included DenseNet201 [20], ResNet50 [21], Inception V3 [22], and VGGNet19 [23]. Implemented in Python 3 using Keras v2.6 [24] and TensorFlow v2.6 [25] code libraries, with parameters specified in Table 3.

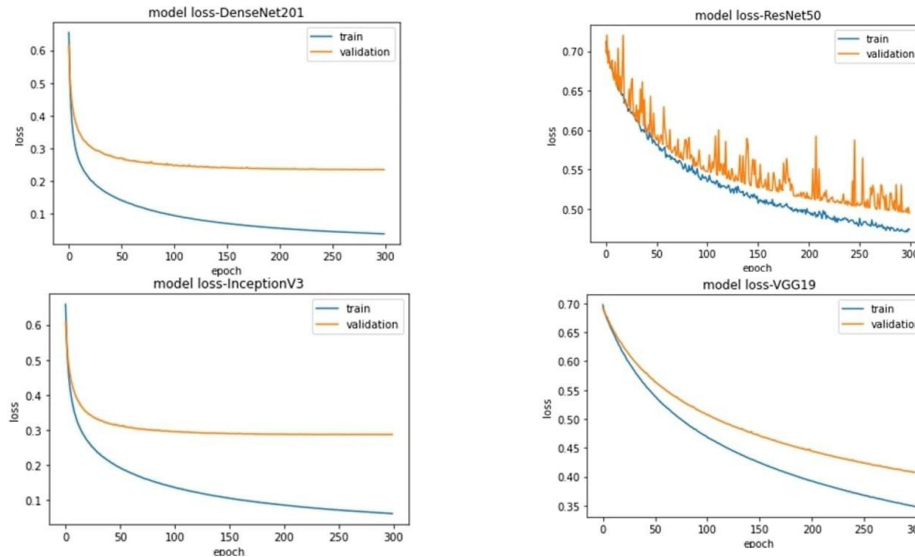
Table 3. Parameter settings for CNN model evaluations

Parameters	Value	Remark
TEST EPOCH	30	The number of test epochs
IMAGE_SIZE	224 x 224	Input images for all models
BATCH_SIZE	32	Size of the dataset to test the models for each epoch
MODEL_EPOCH	300	Number of tests
ACTIVATION_FUNCTION	SIGMOID	Suitable for two classes with data in 0, 1
OPTIMIZERS	SGD	Stochastic gradient descent (SGD) is a fast algorithm which updates parameters at each training step.
LOSS FUNCTION	BINARY_CROSSENTROPY	There are only two classes in this research.

Figure 15(A) shows the model learning behavior in terms of accuracy over all epochs, as a learning model comparison between DenseNet201, ResNet50, Inception V3, and VGGNet19. Figure 15(B) shows each model’s loss function behavior over all epochs. The results illustrate that DenseNet201 achieves the highest learning accuracy, and has the least validation loss, with relatively low overfitting between training and validation image sets.



(A) Accuracy of DenseNet201, ResNet50, Inception V3, and VGGNet19



(B) Loss rate of DenseNet201, ResNet50, Inception V3, and VGGNet19

Figure 15. The comparison of the learning model of CNNs

Table 4 summarizes the learning performance of all pretrained CNN models on the test dataset. As the dataset classes are equally balanced, the accuracy metric is a reliable performance measure. Every CNN model performs better than random (i.e., can recognize more than 50% of the fungal disease patterns). The model with the highest accuracy in discriminating fungal disease patterns from non-disease patterns is DenseNet201 at 89.74%. The InceptionV3 model accuracy is second in the order at 87.25%. Others (VGGNet19 and ResNet50) are 83.49% and 74.25%, respectively.

Table 4. Comparison of different CNNs fungal disease classification efficiency

CNN model name	Class	Accuracy	Precision	Recall	F1
DenseNet201	Disease	89.74	91.45	90.25	91.48
	Non-Disease		90.57	92.70	91.74
ResNet50	Disease	74.25	74.20	75.25	75.23
	Non-Disease		75.24	74.27	74.25
InceptionV3	Disease	87.25	88.25	85.20	87.26
	Non-Disease		86.23	88.15	87.25
VGGNet19	Disease	83.49	81.41	86.49	84.45
	Non-Disease		86.42	80.40	83.49

Therefore, from these results, DenseNet201 is the most suitable CNN model for the detection and prognosis of mushroom fungal disease in our intelligent farm system.

2.5 Procedure for real-time fungal disease prognosis

Experiments in Section 2.4 show that DenseNet201 is the most accurate model for classifying fungal disease for our dataset, as captured by the imaging robot. Therefore, this model for fungal disease detection (prognosis) is selected to evaluate images from the intelligent farm system in real-time. Figure 16 consists of three steps: (i) image retrieval, (ii) Mask R-CNN image segmentation process, and (iii) fungal disease detection with alerting.

First, the image preparation process retrieves the file paths to recent images recorded by the imaging robot's camera(s). The imaging robot uses a file naming convention with current date and time, such as 17-02-2022T14:39:04 (DD-MM-YYYYThh:mm:ss). Each image is sent individually into the Mask R-CNN process for segmentation (cropping). The cropped image has a fixed size of 224 x 224 pixels. The image preparation process is executed within its own Python virtual environment, v1.2 [26].

The newly cropped image's path is transferred to a prognostic process (DenseNet201) to evaluate whether the cropped mushroom image contains fungal disease or no disease. The prognostic results are expressed as a percentage (%) of fungal incidence, and directly align to the model's classification percentage (for the disease class).

If the prognostic result exceeds 50% (indicating fungal disease is present), then the system will immediately alert the farmer. The alert sensitivity value can be adjusted according to the situation.

All three of these processes are executed simultaneously, in real-time on the local computer system within the smart farm control room. The total time taken is approximately 2 min 3 s from the first image captured by the imaging robot to prognosis result and notification sent.

3. Results and Discussion

The three components of research work that are evaluated for their effectiveness are as follows: (i) cultivation environment control, (ii) imaging robot positioning and data transmission (i.e., image capture quality) and (iii) fungal disease detection and reporting.

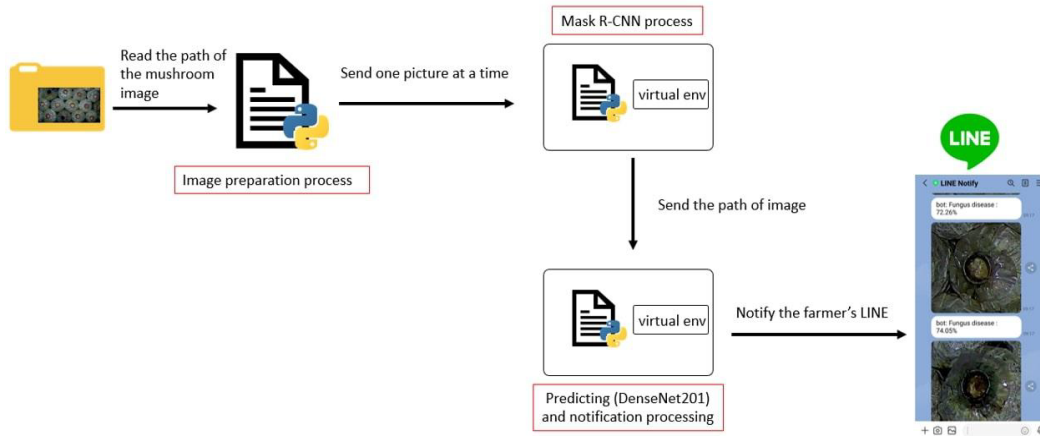


Figure 16. Real-time fungal disease detection/prognosis process, approx. 2:03 min per image cycle

3.1 Evaluation of environment control system for mushroom cultivation

Mushrooms thrive on suitable temperature and humidity levels and do not require light. The best practice cultivation conditions for temperature, relative humidity, light and planting bag moisture varied slightly among our Sajor-caju mushroom consultant farmers. However, an inclusive and acceptable range of conditions was agreed upon for the intelligent farm system data collection trial, as shown in Table 5. The operating trial period was over the months of April to July 2022, and where collected data was trimmed to 91 days (1st-1st). The remaining three sensor categories are positioned on or near to the mushroom racks, and specific sensor components are as stated in Section 2.2.

The sensor values of the environmental control system were measured and recorded as a moving average at a precision granularity of 5-min intervals. Specifically, a data point was recorded as the mean average (sensor) value over the previous 5 min for a given sensor category, from the available sensors in the data trial building. Each data point represents the status across the fruiting chamber. Measured capability (%) in Table 5 reports the percentage of 5-min intervals that fell within the acceptable condition range over the data trial period. It was noted that the control system initiated the misting and fan actuators with the objective to retain the moving average temperature and humidity sensor values within the acceptable ranges.

Table 5. Evaluation trial of environment control system for Sajor-caju mushroom cultivation.

No .	Environment Sensor Category (unit)	Acceptable Condition Range	Measured Capability (%)
1.	Temperature (Celsius: °C)	25-30 °C	100
2.	Humidity (Percentage: %)	60-70 %	100
3.	Lighting (%)	20 – 30 %	100
4.	Moisture in the planting bag (%)	60 – 70 %	98.5
	Overall		99.6

The experimental results in Table 5 show that the environment control for this innovative farm system component performed well over the trial period, with an overall capability of 99.6%,

over 26208 data points (91 days). The moisture in the planting bag (%), which can be thought of as localized humidity, was reported as a capability loss of 1.4995%, or 393 unique time-intervals (32.75 h) outside of the acceptable range. Some loss was expected, as its sensor value change is a by-product of (not directly controlled by) the control system. Further, localized humidity varies over time and across the cultivation racks (as water drains and passes the sensor, etc.); control at this granularity remains open to future work.

3.2 Evaluation of imaging robot

The primary function of the imaging robot is to collect images of the front of each mushroom bag and transfer those images to the service for fungal disease detection. Therefore, the imaging robot's motion, imaging, and image transmission capabilities are evaluated, as shown in Table 6. Percentages of successful operations are reported, i.e., did not exceed the stated error condition.

Measurements of the robot's operations were collected over multiple day-time trial periods to verify that the programmed tasks were completed as intended. One thousand data points per category were recorded. Positioning in X and Y-axes (1,2) and speed control (5) were concerned with capture image framing. Compliance of (1,2) were measured as the distance of the robot's stopping point from each expected position, dictated by the "square wave" pattern cycle. Movement speed control (5) was a measure of the consistency of time taken to complete each pattern cycle; this measurement was concerned with model drift, as caused by inertia or mechanical (mobility) faults such as rail traction and belt operation problems.

Table 6. Performance analysis of imaging robot

No.	Operation of Imaging Robot	Error Condition	Success Rate Operation (%)
1.	Ability to precise position in X-axis	±2 cm	99.8
2.	Ability to precise position in Y-axis	±2 cm	99.6
3.	Ability to capture images	0 images	100
4.	Lighting control for robot photography	0 images	100
5.	Movement speed control in both X and Y axes	±5 seconds	99.5
6.	Ability to transmit image data	0 images	99.4
	Overall		99.7

Image capture ability (3) was measured by the quantity of image capture events per square wave cycle (against the 12 expected), and lighting control (4) error was recorded when a capture event was not illuminated. Similarly, image data transmission (6) was measured by the quantity of image files created in the remote directory (transmitted via wireless communication).

The results in Table 6 show that the overall operational efficiency of the imaging robot during the verification trial was 99.7%. There was some minor loss in motion and position operations (1,2 and 5), which remains open to further control improvement. There was also minor loss in data transmission of image files (99.4%), which we believe was caused by frequency signal disturbances, (such as during high humidity periods or signal interruptions from other devices), or related to receiver-transmitter distance variations during robot traversals.

3.3 Evaluation of real-time fungal disease prognosis system

The real-time fungal disease prognosis system (Figure 16) analyzes captured images of the front of the mushroom planting bags to determine whether fungal disease is present (see Section 2.4); if so, a warning notification is delivered (see Section 2.5). The prognosis (detection) label correctness and notification correctness are imperative to the prognosis system's success. Therefore, the prognosis system's output images and labels were collected after a 1-month period of real-time operation and 13,500 images were retrieved. Each image (224 x 224 pixels) was cropped (segmented) and labeled (by the DenseNet201 CNN model), and then those image labels were individually verified. The resultant (large) test dataset was re-evaluated by the previously trained DenseNet201 (under test) to reproduce the measured performance of the actual real-time prognosis system during that period. Table 7 reports those results. Of most interest is the fungal disease category (positive prognosis), with precision of 94.35%, the recall with 83.98%, and the F1 with 89.47%. The F1 metric equation is a balanced measurement of precision and recall factors, which dropped by 2.01%, from 91.48% (early test trial, n=400) to 89.47% (real-time test trial, n=13500).

Table 7. Real-time fungal disease prognosis results

	Precision (%)	Recall (%)	F1 (%)
Disease	94.35	83.98	89.47
No disease	86.24	93.86	90.35

4. Conclusions

A major source of concern for professional mushroom cultivation farmers is the production cost of crop contamination or crop loss caused by a fungal disease. Inhalation of mushroom spores, like fungal disease spores, directly affects farmer health. Thus, automation of crop inspections with cultivation environment control helps to mitigate both concerns and is the subject of this research – *an innovative and intelligent farm system*. The automated system consists of three parts: (i) an intelligent environment control farm component, (ii) an imaging robot, and (iii) a real-time fungal disease prognosis and early warning system. Each component was evaluated.

The environment control results reported 99.6% measured capability to retain well-defined nominal range conditions over 3-months, which we regard as *precise control* and *excellent* capability performance for Sajor-caju mushroom cultivation. The imaging robot was verified under trial with overall operational efficiency at 99.7% -- *effective* performance, with very minor losses in motion, position control and wireless data transmission. The real-time prognosis and alert system for fungal disease performance over a 1-month dataset was verified at 89.47% F1 score (94.35% precision), marking a minor overall drop of ~2%, from its initially trained-test conditions. While improvements per component were identified as the research proceeded, we regard these controlled trial results as evidence of *excellent* overall performance by the complete and automated system.

The developed system now operates twice daily during the daylight hours, which allows it to identify fungal disease typically within the 6 to 12-h growth-phase and avoids impeding the other farm operations. The farmers can reduce their time exposed to health-threatening mushroom spores, and more comfortably monitor the prognosis notification images sent to their smartphones, and check the farm surveillance videos and software dashboard to track the farm operations and environment status. The early notification, isolation and treatment of fungal disease infections has helped to reduce wide-spread crop loss. Consequently, time-spent replacing mushroom batches is

reduced and therefore savings can begin to increase for year-on-year (replacement) mushroom production costs. Risk of disease, such as lung abscesses, lung diseases, and allergies are further lowered as a result.

In the future, we intend to reapply the proposed system to further mushroom varieties and fungal disease concerns using the racked farm formation, by changing the deep learning image dataset, in order to help alleviate these challenges among more mushroom farmers.

5. Acknowledgements

This research project was financially supported by Mahasarakham University

References

- [1] Stamets, P., 2011. *Growing Gourmet and Medicinal Mushrooms*. California: Ten speed press.
- [2] Chang, S.T. and Wasser, S.P., 2018. Current and future research trends in agricultural and biomedical applications of medicinal mushrooms and mushroom products (review). *International Journal of Medicinal Mushrooms*, 20(12), 1121-1133, <https://doi.org/10.1615/IntJMedMushrooms.2018029378>.
- [3] Alam, N., Amin, R., Khan, A., Ara, I., Shim, M.J., Lee, M. W., Lee, U.Y. and Lee, T.S., 2009. Comparative effects of oyster mushrooms on lipid profile, liver and kidney function in hypercholesterolemic rats. *Mycobiology*, 37(1), 37-42. <https://doi.org/10.4489/MYCO.2009.37.1.037>.
- [4] Mahmud, M.S.A., Buyamin, S., Mokji, M.M. and Abidin, M.S.Z., 2018. Internet of things based smart environmental monitoring for mushroom cultivation. *Indonesian Journal of Electrical Engineering and Computer Science*, 10(3), 847-852. <https://doi.org/10.11591/ijeecs.v10.i3.pp847-852>.
- [5] Raja, S.P., Rozario, A.R., Nagarani, S. and Kavitha, N., 2018. Intelligent mushroom monitoring system. *International Journal of Engineering and Technology*, 7(2.33), 1238-1242.
- [6] Khummanee, S., Wiangsamut, S., Sorntepa P. and Jaiboon C., 2018. Automated smart farming for orchids with the internet of things and fuzzy logic. *International Conference on Information Technology (InCIT)*, Khon Kaen, Thailand, December 24-26, 2018, pp. 1-6.
- [7] Wiangsamut, S., Phatthanaphong, C. and Suchart, K., 2019. Chatting with plants (orchids) in automated smart farming using IoT, fuzzy logic and chatbot. *Advances in Science, Technology and Engineering Systems Journal*, 4(5), 163-173.
- [8] Kassim, M. R. M., Harun, A. N., Yusoff, I. M., Mat, I., Kuen, C. P. and Rahmad, N., 2017. Applications of wireless sensor networks in Shiitake mushroom cultivation. *11th International Conference on Sensing Technology*, Sydney, Australia, December 24-26, 2017, pp. 1-6.
- [9] Chieochan, O., Saokaew, A. and Boonchieng, E., 2017. IOT for smart farm: A case study of the Lingzhi mushroom farm at Maejo University. *14th International Joint Conference on Computer Science and Software Engineering (JCSSE)*, NakhonSiThammarat, Thailand, July 12-14, 2017, pp. 1-6.
- [10] Sorenson, W.G., 1999. Fungal spores: hazardous to health? *Environmental Health Perspectives*, 107(Suppl 3), 469-472, <https://doi.org/10.1289/ehp.99107s3469>.
- [11] Beyers, D., 2023. *Green Mold of Mushrooms*. [online] Available at: <https://extension.psu.edu/green-mold-of-mushrooms>.
- [12] Tinkercad, 2022. *Autodesk Tinkercad*. [online] Available at: <https://www.tinkercad.com>.
- [13] Yang, K., Han, Y., Ma, Y. and Yang, L., 2017. The design and implement of monitoring system for mushroom greenhouses based on intelligent agriculture. *International Conference*

- on Computer Systems, Electronics and Control (ICCSEC)*, Dalian, China, December 25-27, 2017, pp. 695-699.
- [14] Ghavate, S. and Joshi, H., 2020. Smart Farming using IoT and Machine Learning with Image. [online] Available at: <https://easychair.org/publications/preprint/w3Sg>.
- [15] Pooja, V., Das, R. and Kanchana, V., 2017. Identification of plant leaf diseases using image processing techniques. *IEEE Technological Innovations in ICT for Agriculture and Rural Development (TIAR)*, Chennai, India, April 7-8, 2017, pp. 130-133.
- [16] Girshick, R., Donahue, J., Darrell, T. and Malik, J., 2014. Rich feature hierarchies for accurate object detection and semantic segmentation. *Proceedings of the IEEE Conference on Computer Vision and Pattern Recognition*, Columbus, USA, June 23-28, 2014, pp. 580-587.
- [17] Jin, X-B., Yu, X-H., Wang, X-Y., Bai, Y-T., Su, T-L. and Kong, J-L., 2020. Deep learning predictor for sustainable precision agriculture based on internet of things system. *Journal of Sustainability*, 12(4), <https://doi.org/10.3390/su12041433>.
- [18] Noe, S.M., Zin, T.T., Tin, P. and Kobayashi, I., 2022. Automatic detection and tracking of mounting behavior in cattle using a deep learning-based instance segmentation model. *International Journal of Innovative Computing, Information and Control*, 18(1), 18211-18220.
- [19] Gandhi, R., 2018. *R-CNN, Fast R-CNN, Faster R-CNN, YOLO Object Detection Algorithms*. [online] Available at: <https://towardsdatascience.com/r-cnn-fast-r-cnn-faster-r-cnn-yolo-object-detection-algorithms-36d53571365e>.
- [20] Huang, G., Liu, Z., Maaten, L.V.D. and Weinberger, K.Q., 2017. Densely connected convolutional networks. *Proceedings of the IEEE Conference on Computer Vision and Pattern Recognition*, Honolulu, USA, July 21-26, 2017, pp. 4700-4708.
- [21] He, K., Zhang, X., Ren, S. and Sun, J., 2016. Deep residual learning for image recognition. *Proceedings of the IEEE Conference on Computer Vision and Pattern Recognition*, Las Vegas, USA, June 27-30, 2016, pp. 770-778.
- [22] Szegedy, C., Vanhoucke, V., Ioffe, S., Shlens, J. and Wojna, Z., 2016. Rethinking the inception architecture for computer vision. *Proceedings of the IEEE Conference on Computer Vision and Pattern Recognition*, Las Vegas, USA, June 27-30, 2016, pp. 2818-2826.
- [23] Simonyan, K. and Zisserman, A., 2014. *Very Deep Convolutional Networks for Large-scale Image Recognition*. [online] Available at: <https://arxiv.org/abs/1409.1556>.
- [24] Chollet, F., 2022. *About Keras*. [online] Available at: <https://keras.io>.
- [25] Google, 2022. *TensorFlow*. [online] Available at: <https://www.tensorflow.org>.
- [26] Dataquest, 2022. *A Complete Guide to Python Virtual Environments*. [online] Available at: <https://www.dataquest.io/blog/a-complete-guide-to-python-virtual-environments/>.